

# A Broad-Spectrum Antimicrobial and Antiviral Membrane Inactivates SARS-CoV-2 in Minutes

Qingsheng Liu, Yidan Zhang, Wanjun Liu, Long-Hai Wang, Young W. Choi, Megan Fulton, Stephanie Fuchs, Kaavian Shariati, Mingyu Qiao, Victorien Bernat, and Minglin Ma\*

SARS-CoV-2, the virus that caused the COVID-19 pandemic, can remain viable and infectious on surfaces for days, posing a potential risk for fomite transmission. Liquid-based disinfectants, such as chlorine-based ones, have played an indispensable role in decontaminating surfaces but they do not provide prolonged protection from recontamination. Here a safe, inexpensive, and scalable membrane with covalently immobilized chlorine, large surface area, and fast wetting that exhibits long-lasting, exceptional killing efficacy against a broad spectrum of bacteria and viruses is reported. The membrane achieves a more than 6 log reduction within several minutes against all five bacterial strains tested, including gram-positive, gram-negative, and drugresistant ones as well as a clinical bacterial cocktail. The membrane also efficiently deactivated nonenveloped and enveloped viruses in minutes. In particular, a 5.17 log reduction is achieved against SARS-CoV-2 after only 10 min of contact with the membrane. This membrane may be used on hightouch surfaces in healthcare and other public facilities or in air filters and personal protective equipment to provide continuous protection and minimize transmission risks.

Q. Liu, W. Liu, L.-H. Wang, S. Fuchs, K. Shariati, M. Ma Department of Biological and Environmental Engineering Cornell University Ithaca, NY 14853, USA E-mail: mm826@cornell.edu Y. Zhang Department of Fiber Science and Apparel Design Cornell University Ithaca, NY 14853, USA Y. Zhang, M. Qiao Halomine Inc. Ithaca, NY 14853, USA Y. W. Choi, M. Fulton Battelle Memorial Institute Columbus, OH 43201, USA Department of Materials Science and Engineering Cornell University Ithaca, NY 14853, USA

The ORCID identification number(s) for the author(s) of this article can be found under https://doi.org/10.1002/adfm.202103477.

DOI: 10.1002/adfm.202103477

#### 1. Introduction

The COVID-19 pandemic, caused by the severe acute respiratory syndrome coronavirus 2 (SARS-CoV-2), has infected more than 172 million people and resulted in more than 3.7 million deaths worldwide since its outbreak. Studies have shown that SARS-CoV-2 remains viable and infectious in aerosols for hours and on surfaces for days.[1] As a result, on top of social distancing and mask-wearing, frequent surface decontamination becomes one of the most important preventative measures to minimize transmission risks.[2] Traditional, liquid-based disinfectants such as chlorinebased products, have been widely used during this pandemic due to their antiviral potency and history of relatively safe use.[3] However, they decontaminate the surface only at time of application and provide no long-lasting protection after evaporation. In other efforts, copper-based surfaces or those coated with polymeric quaternary

ammonium compounds, have prolonged antiviral properties.<sup>[1c,4]</sup> However, these surfaces often require drying or long contact time (hour scale) with the viral contaminants to be effectively antiviral.

Here, we report a robust, safe, inexpensive, and scalable membrane with long-lasting, exceptional killing efficacy against a broad spectrum of bacteria and viruses. In particular, the membrane inactivates SARS-CoV-2 with an over 5 log reduction after only 10 min of contact. We designed this anti-viral membrane (AVM) based on three desirable attributes: 1) a potent and safe antiviral agent that can be stably incorporated into the membrane; 2) a large surface to volume ratio to maximize the immobilization of the antiviral agent on the surface of the membrane; and 3) high wettability to promote rapid and intimate contact with viral contaminants for effective contact killing. To develop such an AVM, we designed and synthesized two miscible polyurethanes, one with a hydantoin side group which can covalently bond and stably immobilize oxidative chlorine<sup>[5]</sup> and one with a zwitterionic group that imparts hydrophilicity<sup>[6]</sup> and promotes fast wetting. We then used electrospinning to make the sub-micron fibrous membrane from the polyurethane blends. The sub-micron fibrous structures provide a large surface area  $(\approx 10 \text{ m}^2 \text{ g}^{-1})^{[7]}$  for chlorine immobilization and also enhance

www.afm-iournal.de

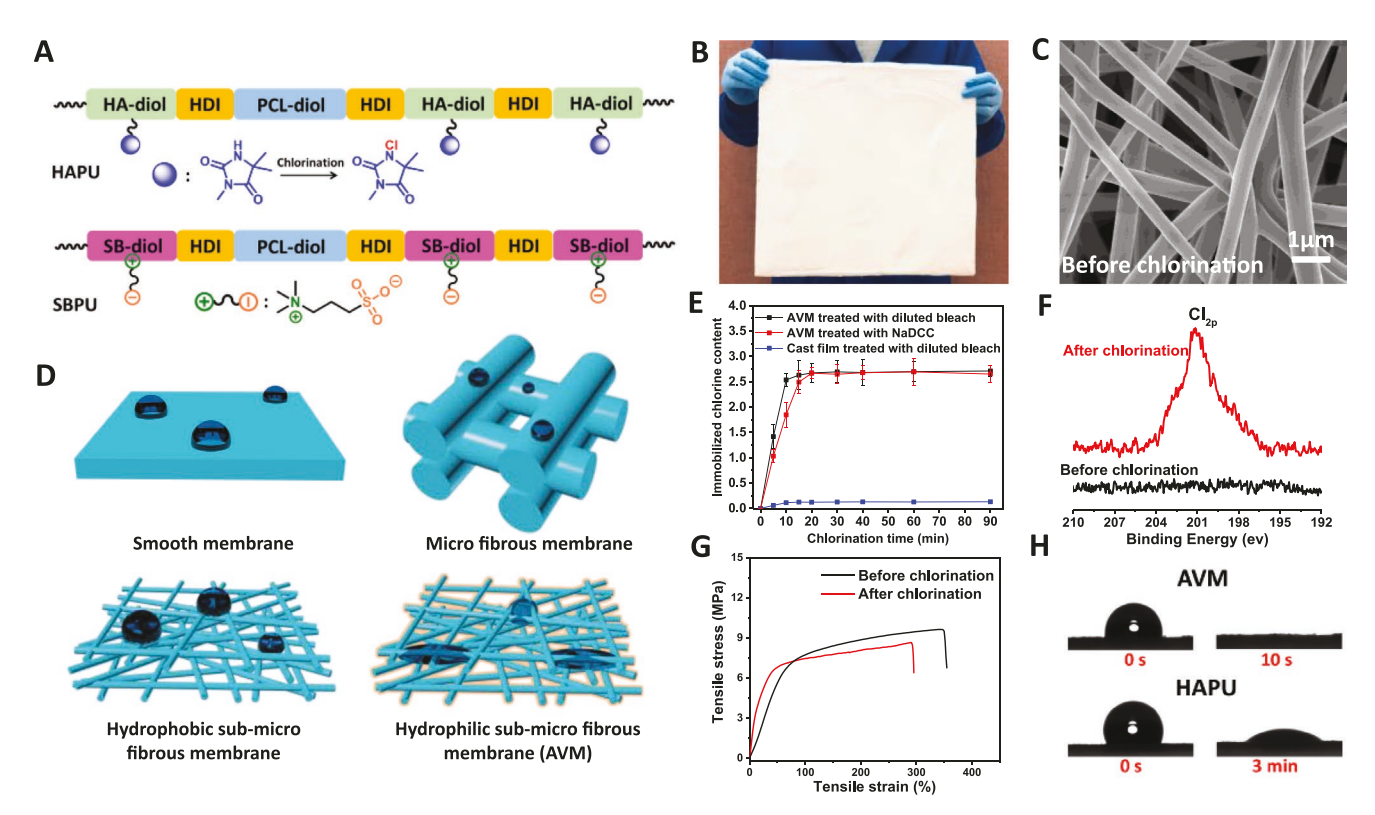


Figure 1. Design, fabrication and characterization of the AVM. A) Schematic illustration of the two polyurethanes, HAPU and SBPU. B) A photograph of the membrane made of HAPU and SBPU. C) SEM image of the membrane made of HAPU and SBPU before chlorination. D) Schematic illustrations of respiratory droplets on smooth, micro fibrous, hydrophobic sub-micro fibrous, and hydrophilic sub-micro fibrous membranes. E) Immobilized chlorine content (weight percentage) of AVM and cast film as a function of chlorination time. F) XPS Cl 2p spectra of the membranes made of HAPU and SBPU, before and after chlorination. G) Stress—strain curves in tensile test for the membranes made of HAPU and SBPU, before and after chlorination. H) Digital photographs of water droplets on AVM and HAPU membranes.

wetting even for small size, respiratory droplets. To prepare the membrane for use, it was treated with a household chlorinebased disinfectant, rinsed to remove any free chlorine and dried. The AVM exhibits near complete killing with 99.9999% reduction within 1 min of all five bacterial strains tested, including grampositive, gram-negative and drug-resistant ones as well as a clinical bacterial cocktail. The AVM was also tested against enveloped viruses, transmissible gastroenteritis coronavirus (TGEV) and SARS-CoV-2, and non-enveloped feline calicivirus (FCV).[8] No viable TGEV was detectable after just 1 min exposure. Although the non-enveloped FCV was somewhat more resistant, no infectious virus was detectable after 30 min; and 1 and 10 min sufficed to reduce infectivity by 2.17 and 4.72 log, respectively. In particular, a 5.17 log reduction of SARS-CoV-2 was achieved after a 10 min of contact, and no infectious SARS-CoV-2 was detectable after 30 min. The AVM may be attached to high-touch surfaces or used in air filters and personal protective equipment (PPE) to provide continuous protection and minimize transmission risks.

#### 2. Results

#### 2.1. Design, Fabrication, and Characterization of AVM

We chose polyurethanes as the base material because they are inexpensive, easy to scale, widely used, and tunable to

form a wide array of materials from soft elastomers to rigid plastics.<sup>[9]</sup> To synthesize the polyurethane with the hydantoin group (namely HAPU) and the one with the zwitterionic sulfobetaine group (namely SBPU), HA-diol, and SB-diol based monomers, respectively, were first prepared and confirmed by NMR (Figure S1, Supporting Information) A polycaprolactone diol (PCL-diol) with a molecular weight of 2 kDa was used as a soft, elastic segment of the polyurethanes, while a 1, 6-Diisocyanatohexane (HDI) was used as building blocks. The synthesis of HA based polyurethane (HAPU) and SB based polyurethane (SBPU, Figure 1A) were carried out according to the schemes as shown in Figure S2, Supporting Information, and characterized as shown in Figure S3, Supporting Information. We then blended HAPU and SBPU (mass ratio of HAPU and SBPU = 3:1) and used electrospinning to fabricate the membrane containing both HA and SB groups (Figure 1B,C and Figure S4, Supporting Information). The fiber diameter (≈0.6–0.9 µm) and average pore size (≈0.8–2.8 µm) of the membrane was tuned by adjusting the polyurethane concentration (Figures S5 and S6, Supporting Information). It is important to note that the hydrophilic, sub-micro fibrous structure is highly effective to promote wetting even when exposed to small size, respiratory droplets (submicron to hundreds of microns)[10] which may not wet as readily smooth membranes, microfibrous membranes or hydrophobic sub-micro fibrous membranes (Figure 1D).

www.advancedsciencenews.com www.afm-journal.de

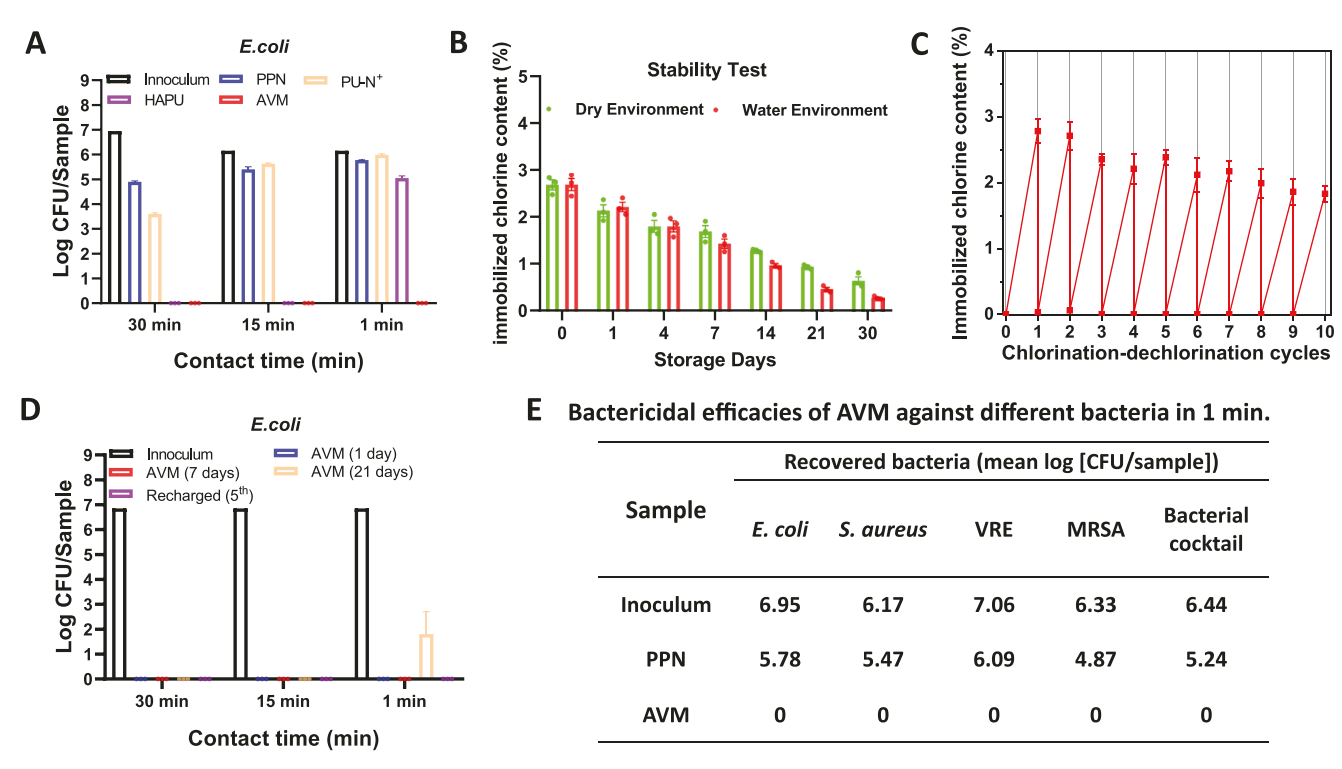


**Figure 2.** AVM rapidly and efficiently inactivates a broad spectrum of bacteria. A) Viable *E. coli* on AVM, PPN, HAPU, as well as PU-N<sup>+</sup> membranes after different contact time. B) Stability of immobilized chlorine (weight percentage) on AVM under dry or aqueous condition. C) Immobilized chlorine content on AVM after 10 chlorination—dechlorination cycles. D) Viable *E. coli* on the AVM with different shelf times or recharged for the 5th time. E) Bactericidal efficacies of AVM against *S. aureus*, VRE, MRSA, and the bacterial cocktail after 1 min of contact, with PPN as a control.

The membrane has a high chlorine loading capacity. After treatment with a diluted household bleach or other halogenating agents such sodium dichloroisocyanurate (NaDCC) (used for the sterilization of swimming pool and drinking water), the N-H group on the membrane surface was transformed into N-Cl (N-halamine) structure. The chlorine content, measured via an iodometric titration method, increased with chlorination time (Figure 1E), saturating at ≈2.63% (w/w) after 15 min. The chlorine content was almost 20 times more than that of a cast film made from the same polyurethane blend. The XPS spectrum (Figure 1F) revealed a peak at 201 eV, attributable to Cl 2p, indicating the formation of N-halamine (N-Cl) groups after chlorination. In addition, XPS signals (Figure S7A, Supporting Information) at 403 and 168 eV from nitrogen and sulfur, respectively, confirmed the existence of SB group on the membrane. The chlorinated membrane or AVM was mechanically robust with a tensile strength of ≈8.6 MPa at a strain of ≈295%, slightly lower than before chlorination (Figure 1G). Moreover, like the untreated membrane, the chlorinated one presented excellent thermal stability (Figure S7B, Supporting Information). Lastly, the AVM and SBPU membrane (Figure S8, Supporting Information) were highly wettable with water droplets quickly spreading and becoming imbibed into the membrane within 10 s. In contrast, a water droplet maintained a contact angle after 3 min on the membrane made of HAPU alone (also chlorinated) (Figure 1H). The fast wetting is important to facilitate intimate contact with viruses inside a respiratory droplet. The large amount of immobilized chlorine and fast wetting make the AVM an ideal candidate to inactivate viruses and

bacteria. Furthermore, MTT assays (Figure S9, Supporting Information) revealed negligible cytotoxicity of the AVM membrane, confirming its safety.

#### 2.2. Anti-Bacterial Properties of AVM

AVMs were prepared and used 7 days after chlorination unless noted otherwise. We first evaluated the bactericidal effect via a direct contact method against five model strains: gramnegative Escherichia coli, gram-positive Staphylococcus aureus, vancomycin-resistant Enterococci (VRE), methicillin-resistant S. aureus (MRSA), and a clinically isolated cocktail of 14 strains (see Table S1, Supporting Information, for details). In addition, to better assess the bactericidal effect of AVM (chlorinated;  $1.68 \pm 0.13\%$  chlorine content) we included 3 controls: a polypropylene non-woven (PPN) membrane (a primary material used in the manufacture of PPE[11]), a sub-micron fibrous membrane made of HAPU alone (also chlorinated; 1.74 ± 0.09% chlorine content), and a sub-micron fibrous membrane made of another type of polyurethane with quaternary amine groups (namely PU-N+ membrane) which is known to be effective at inactivating bacteria.[12] About 4.89 log colony forming units per sample (CFU/sample) of E. coli remained on the surface of PPN after 30 min of contact (Figure 2A). In contrast, AVM and HAPU membranes inactivated all inoculated bacteria, whereas there was 3.61 log CFU/sample of E. coli remaining on the PU-N+ membrane. More drastic differences started to emerge as the contact time was decreased. At 15 min, no viable





www.afm-journal.de

bacteria were detected on AVM or HAPU membranes, but 5.63 log CFU/sample remained on the PU-N<sup>+</sup> membrane. At 1 min, still no viable bacteria were detected on AVM, a 6-log reduction or a bactericidal efficacy of 99.9999%, whereas neither PU-N<sup>+</sup> nor HAPU membranes had significant bactericidal effect at this short exposure (Figure 2A). These results showed superior bactericidal effects of AVM compared to PU-N<sup>+</sup> or HAPU membranes, likely resulting from the combination of large content of potent chlorine and high wettability of AVM.

Next, we investigated the stability and reusability of the AVM in bacteria killing. The chlorine content of AVM gradually decreased over time under dry condition (25 °C, 15-20% relative humidity) and in water, but the decrease was slow and 25% of initial chlorine content remained in dry condition after 30 days (Figure 2B). Furthermore, the AVMs used in this study were made from one batch of SBPU and four different batches of HAPU. The content and stability of immobilized chlorine on the AVM made from each batch was consistent (Figure S10, Supporting Information). Furthermore, the chlorine content of the AVM could be replenished using a household bleach solution for at least 10 chlorination-dechlorination (quenching) cycles (Figure 2C). We tested the bactericidal effect of AVM, 1, 7, and 21 days after chlorination (corresponding to 2.12%, 1.68%, and 0.94% chlorine content, respectively) or recharged for the 5th time. Similar biocidal efficacy of 99.9999% for 2 h or 30 min contact time was observed in all cases (Figure 2D). Only 1.80 log CFU/sample of E. coli was detected on the 21-day old AVM after 1 min exposure, while no bacteria could be detected in any other case. Lastly, when inoculated with S. aureus, VRE, MRSA, and the bacterial cocktail, the AVM exhibited similarly robust and ultra-fast biocidal performances (Figure 2E, Figure S11 and Table S2, Supporting Information), achieving more than 6 log CFU reduction within 1 min of contact, in contrast to other antimicrobial membranes which usually required a contact of 30 min to several hours to achieve up to 4 log CFU reduction.[13] All these data showed that the AVM had stable, superior bactericidal effects against a broad spectrum of bacteria for practical uses.

#### 2.3. Anti-Viral Properties of AVM

The most impactful application of AVM during this pandemic would be inactivation of SARS-CoV-2.[14] Therefore, we evaluated the antiviral activity of AVM against different viruses including SARS-CoV-2. We first chose a FCV, a surrogate for human norovirus<sup>[15]</sup> which is a leading cause of acute gastroenteritis worldwide. FCV is a non-enveloped, single stranded, positive sense RNA virus. Non-enveloped viruses are typically more resistant to disinfectants and other stresses like heat or drying than enveloped ones.[16] We analyzed the antiviral activity of AVM against 100  $\mu$ L FCV (2.92  $\times$  10<sup>6</sup> TCID<sub>50</sub>/sample) deposited in 10 separate droplets onto the surface of AVM or PPN (control). Infectious FCV loads remaining on each surface after pre-determined contact periods were quantified on Crandell-Reel feline kidney (CRFK) cells by the 50% tissue culture infective dose (TCID<sub>50</sub>) method. Cytopathic effects (CPE) were observed under microscope and confirmed after crystal violet staining. While  $2.75 \times 10^5 \text{ TCID}_{50}/\text{sample}$  of FCV were recovered from PPN membrane after a 2-h exposure, no CPE was observed either under microscope or under visual inspection in the AVM group (Figure S12, Supporting Information), implying a more than 4.1 log reduction in infectivity in comparison to PPN (**Figure 3**A). Similar results were obtained after 30 min of contact. Decreasing contact time to 10 or 1 min led to almost no virus reduction on PPN membrane, while the AVM reduced the virus titer from  $10^{6.47}$  to  $10^{1.75}$  TCID<sub>50</sub>/sample in 10 min, or from  $10^{6.24}$  to  $10^{4.07}$  (99.3% inactivation) in just 1 min.

We then compared AVM with HAPU and PU-N+ membranes in FCV inactivation. While the PU-N+ membrane had certain antiviral effect, the AVM performed much better with at least 1.37, 1.84, and 2.71 more log reductions after 120-, 30-, and 10-min contact, respectively (Figure 3B). We concluded that N-halamine based AVM was more potent against FCV than the quaternary amine-based membrane. In comparison with the HAPU membrane with identical chlorine content, the AVM lowered the virus titers by 1.09, 2.84, and 2.54 more logs after 120-, 30-, and 10-min contact, respectively. These data confirmed again the importance of the zwitterionic SBPU component that imparted hydrophilicity into the AVM and promoted rapid interactions between the membrane surface and virus, leading to enhanced antiviral performance compared to the relatively hydrophobic HAPU membrane. Moreover, as expected, the membrane made of HAPU and SBPU without chlorination had no anti-viral effect (Figure S13A, Supporting Information).

We also tested the FCV inactivation by the AVM after 1, 7, and 21 days of shelf time. No viable FCV was detected on any of the three sets of membranes after 30 min or 2 h contact (Figure 3C and Figure S13B, Supporting Information). When the contact time was shortened to 10 min, the FCV titer on 1-day old AVM was reduced from 6.47 to 1.43 log(TCID<sub>50</sub>/ sample); and to 1.70 log(TCID<sub>50</sub>/sample) or 3.53 log(TCID<sub>50</sub>/ sample) on 7 and 21 day old AVMs, respectively. These results indicated that the 21-day-old AVM had potent antiviral activity after contact as short as 10 min. In addition, AVM after five cycles of quenching/chlorination still maintained robust antiviral behavior (Figure 3C), which was comparable to the AVM after first chlorination. Even stronger potency was observed against the TGEV, an enveloped, positive-sense, single-stranded RNA virus from genus Alphacoronavirus, subgenus Tegacovirus, chosen as a surrogate for other pathogenic human coronavirus such as SARS-CoV-1. [17] A lower titer of TGEV ( $2.8 \times 10^4$ TCID<sub>50</sub>/sample) was applied to the AVM using the same protocol as for FCV. No viable TGEV was detected on the AVM after as short as 1-min contact (Figure 3D), while significant infectivity was recovered from the PPN control after all contact times. AVM with various shelf time or recharged all retained the activity against TGEV (Figure 3E and Figure S14, Supporting Information).

# 2.4. Inactivation of SARS-CoV-2

Most significantly, the AVM was similarly effective in inactivating the SARS-CoV-2 that caused this pandemic. AVM was prepared at Cornell University and 7 days later shipped overnight to Battelle Memorial Institute for SARS-CoV-2 testing. We applied a total volume of 100  $\mu L$  inoculum containing  $7.8 \times 10^5$ 

www.advancedsciencenews.com www.afm-journal.de

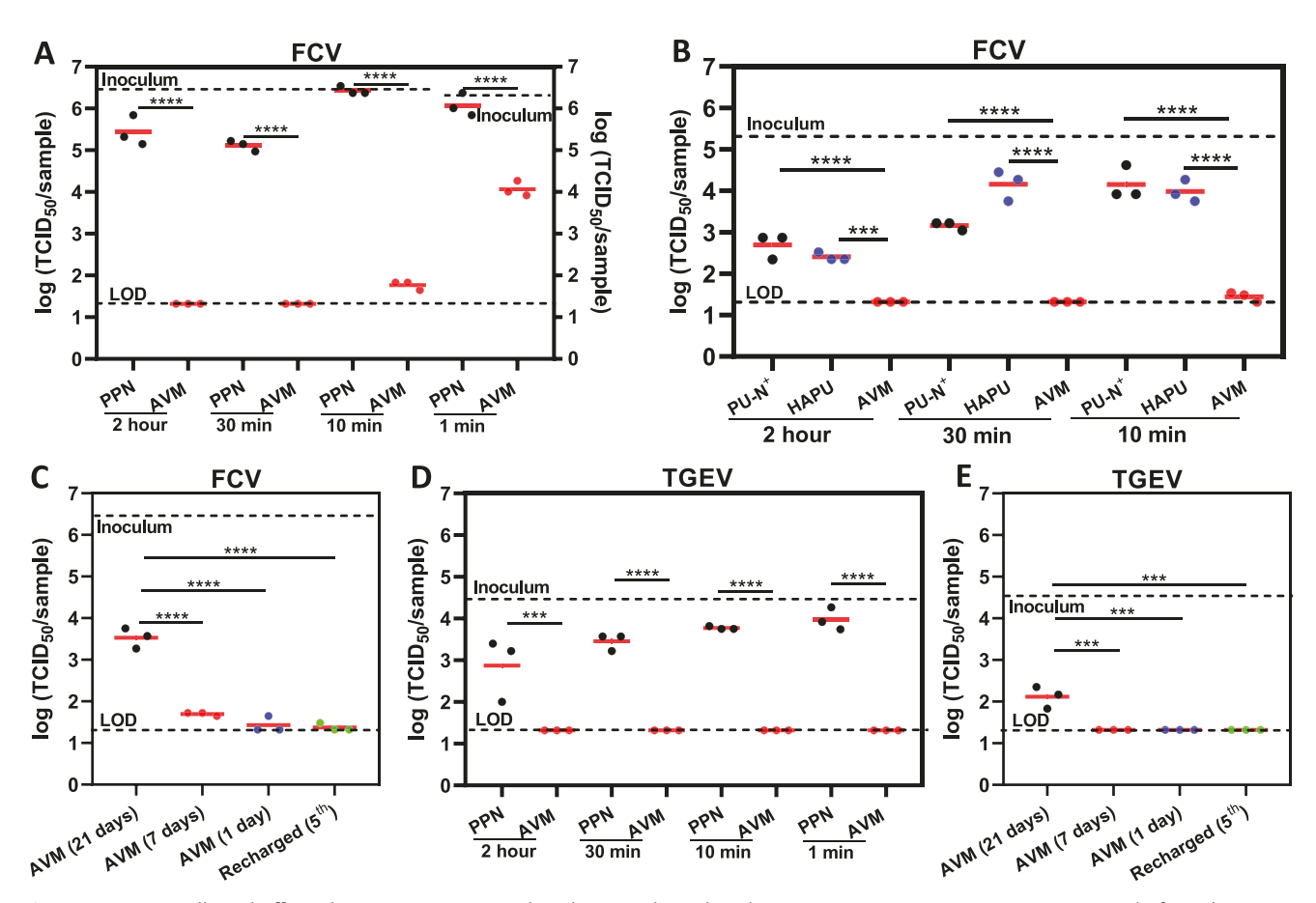


**Figure 3.** AVM rapidly and efficiently inactivates non-enveloped FCV and enveloped TGEV. A) FCV titer on AVM or PPN control after 2 h, 30 min, 10 min, and 1 min contact. B) FCV titer on AVM, HAPU, or PU-N<sup>+</sup> after 2 h, 30 min and 10 min contact. C) FCV titer on AVM with different shelf times or recharged for the 5th time after 10 min contact. D) TGEV titer on AVM or PPN control after 2 h, 30 min, 10 min, and 1 min contact. E) TGEV titer on AVM with++ different shelf times or recharged for the 5th time after 10 min contact. LOD: limit of detection for the TCID<sub>50</sub> assay. n = 3 per group. \*\*\*\*p-value < 0.001, and \*\*\*\*p-value < 0.0001.

 $TCID_{50}/sample$  SARS-CoV-2 in 10 separate droplets onto each AVM for 2 h contact. SARS-CoV-2 was completely inactivated within the detection limit (LOD) of the assay (1.42 log[ $TCID_{50}/sample$ ]) (Figure 4A). In contrast, the virus titer on the PPN membrane control was only slightly reduced from 5.89 to 5.39

 $log(TCID_{50}/sample)$ . The viral titer on AVM was reduced by 3.97 log and 99.99% in comparison to the PPN membrane.

Next, we tested shorter contact time and higher viral inoculum. A one hundred microliter bolus containing SARS-CoV-2 ( $6.7 \times 10^6$  TCID<sub>50</sub>/sample) was inoculated in 10 separate

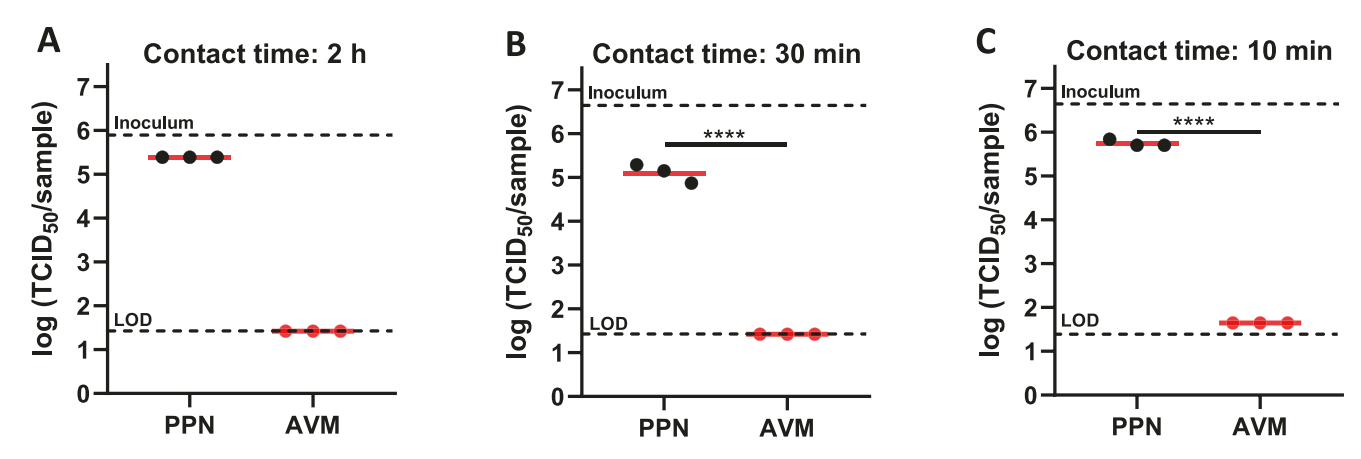


**Figure 4.** AVM rapidly and efficiently inactivates SARS-CoV-2. A) SARS-CoV-2 titer on AVM or PPN membranes after 2 h contact. B) SARS-CoV-2 titer on AVM or PPN membranes after 30 min contact. C) SARS-CoV-2 titer on AVM or PPN membranes after 10 min contact. n = 3 per group. \*\*\*\*\*p-value < 0.0001.



www.afm-iournal.de

Table 1. Virus viability including SARS-CoV-2 on the AVM after different contact time.

Virus	Inoculum [TCID <sub>50</sub> ]	Contact time	Recovery (TCID <sub>50</sub> ) from AVM	Log reduction	% reduction	Recovery (TCID <sub>50</sub> ) from PPN control
SARS-CoV-2	10 <sup>5.89</sup>	120 min	ND	≥4.47	≥99.9966	10 <sup>5.39</sup>
SARS-CoV-2	10 <sup>6.82</sup>	30 min	ND	≥5.40	≥99.9996	10 <sup>5.13</sup>
SARS-CoV-2	10 <sup>6.82</sup>	10 min	101.65	5.17	99.9993	10 <sup>5.76</sup>
FCV	10 <sup>6.47</sup>	120 min	ND	≥5.15	≥99.9993	10 <sup>5.44</sup>
FCV	10 <sup>6.47</sup>	30 min	ND	≥5.15	≥99.9993	10 <sup>5.11</sup>
FCV	10 <sup>6.47</sup>	10 min	10 <sup>1.75</sup>	4.72	99.9981	10 <sup>6.43</sup>
FCV	10 <sup>6.24</sup>	1 min	10 <sup>4.07</sup>	2.17	99.3239	10 <sup>6.09</sup>
TGEV	10 <sup>4.45</sup>	120 min	ND	≥3.13	≥99.9259	10 <sup>2.87</sup>
TGEV	10 <sup>4.45</sup>	30 min	ND	≥3.13	≥99.9259	103.45
TGEV	10 <sup>4.45</sup>	10 min	ND	≥3.13	≥99.9259	103.77
TGEV	10 <sup>4.45</sup>	1 min	ND	≥3.13	≥99.9259	10 <sup>3.98</sup>

Note: ND indicates not detectable.

droplets on AVM and allowed to dwell for 30 min. No viable SARS-CoV-2 on AVM was detected within the LOD (Figure 4B). It yielded more than 3.71 log reduction when compared with the PPN membrane. The contact time was further decreased to 10 min. As expected, a high percentage of viruses was recovered from the PPN control (Figure 4C). In contrast, AVM predictably had an inactivation efficacy at a log reduction of 4.11 compared to PPN. After a mere 10 min, AVM induced viable SARS-CoV-2 titers to decrease from 6.82 log(TCID<sub>50</sub>/sample) to 1.65 log(TCID<sub>50</sub>/sample), leading to a 5.17 log reduction or 99.999% of inactivation. These data, together with those from FCV and TGEV as summarized in Table 1 established the AVM as a superior, broad-spectrum antiviral membrane.

# 3. Discussions

There are several design features in the AVM that contribute to its exceptional killing efficacy against bacteria and viruses. In general, there are two main killing mechanisms: contact killing where inactivation occurs after contact, and release killing where the active agent is released into liquid to inactivate bacteria or viruses.<sup>[5a]</sup> The contact killing was likely the primary mechanism for the AVM since no significant free chlorine (less than 0.1 ppm) was detected in media where AVMs were immersed for 10 min, 30 min, or 2 h and no difference in FCV infectivity was observed when the virus was incubated with the leachates or blank culture medium (Figure S15, Supporting Information). Diluted commercial bleach at the same chlorine concentration (0.1 ppm) was included as control for the antimicrobial and antiviral tests. The results (Figure S16, Supporting Information) indicated that such a low chlorine concentration did not have any significant antimicrobial and antiviral properties. Oxidative chlorine atoms from N-halamine can be transferred onto bacterial or viral membranes upon contact and inactivate them with efficacies dependent on the rate and amount of chlorine transfer.<sup>[5a]</sup> An appropriate *N*-halamine structure with balanced activity and stability is necessary to achieve bacterial or viral inactivation with high and long-lasting

efficacy. The chemical stability of N-halamine decreases from amine to amide to imide N-halamine, while the antimicrobial activity increases in the same order.[5d] Among the amide N-halamines, the one formed by hydantoin group is particularly attractive because of the cyclic structure-enhanced stability and the absence of  $\alpha$ -hydrogen (and hence elimination of HCl). [5a,18] In addition, some of the N-H in urethane bonds can be chlorinated and contribute to the overall chlorine content, although the formed N-halamine tends to be less stable. [19] Besides the hydantoin as the main chlorine immobilizing group, the high surface to volume ratio and thus the amount of N-halamine groups on the surface of AVM also contribute to its stable and high chlorine content. Three weeks after preparation, the AVM still contains ≈0.94% (w/w) active chlorine and the chlorine can be repeatedly replenished as needed.

In addition to high immobilized chlorine content, effective contact killing also requires fast and intimate contacts between the surface and the bacteria or viruses. The hydantoin group and the HAPU polymer are relatively hydrophobic. We thus incorporated into the AVM a zwitterionically modified SBPU. The sulfobetaine is among the most hydrophilic groups because of its zwitterionic nature. [6a,20] The hydrophilicity combined with the highly porous structure of the sub-micron fibrous surface of AVM resulted in the so-called Wenzel state<sup>[21]</sup> and facilitated fast and complete wetting. In particular, even small respiratory droplets which may not readily wet conventional surfaces with features larger than the droplets themselves can still be imbibed into the hydrophilic sub-micron fibrous structure due to capillary action. It is also interesting to note that zwitterionic motifs are also known to form a hydration layer on the surface that acts as a physical and energetic barrier to prevent biofouling. [6a,22] Our experiments indeed showed minimal bacteria attached to the surface of SBPU membranes (Figure S17A, Supporting Information). The amount of dead bacteria attached to the AVM post-killing was on average 20.1% of those attached to the HAPU membranes (Figure S17B, Supporting Information). It should be noted that unchlorinated SBPU membrane was not able to kill virus or bacteria (Figure S18, Supporting Information), although the membrane possessed antifouling





www.afm-journal.de

properties. The unique *N*-halamine group, the zwitterionic chemistry and the sub-micron fibrous structures in the AVM design all played important roles synergistically in achieving the observed antibacterial and antiviral properties.

In design of the AVM, we also considered its practical applications. For example, the synthesis of the polyurethane base material and the manufacturing of the membrane by electrospinning are both tunable, inexpensive, and scalable. Moreover, the antibacterial activity of the AVM was relatively stable after single chlorination (Figure S19, Supporting Information) and under different environmental conditions such as pH and temperature (Figure S20, Supporting Information). Since the AVM is also soft, lightweight, breathable, heat-processable, rechargeable and durable, it may be used in a number of applications. It may be attached using adhesive tapes to high-tough surfaces in healthcare facilities or other public spaces such as doorknobs (Figure S21A, Supporting Information) and shopping cart handles (Figure S21B, Supporting Information) to provide continuous protection. It may be incorporated into PPE using a simple heat press (Figure S20C, Supporting Information), rendering PPE even safer during wear, reuse, or disposal, by adding to it the ability to immediately inactivate infectious pathogens. The AVM may also be used in air and water filters to trap and more importantly kill pathogens (Figure S22, Supporting Information). In summary, the AVM is a broad-spectrum, highly effective and reusable antibacterial and antiviral membrane that can inactivates pathogens including SARS-CoV-2 within minutes and may be capable to provide long-lasting protections during any local outbreak or global pandemic.

#### 4. Experimental Section

Materials: Polycaprolactone diol (Mn 2000, PCL-diol, Sigma-Aldrich) was dried in vacuum oven prior to synthesis. 5,5-dimethylhydantoin, diethanolamine, formaldehyde solution (36.0% in H<sub>2</sub>O), stannous octoate (Sn(Oct)<sub>2</sub>), 1,4-diaminobutane, NaDCC, potassium iodine, anhydrous dimethyl sulfoxide (DMSO), dichloromethane (DCM), diethyl ether, and methanol were purchased from Sigma-Aldrich. N-butyldiethanolamine, 1,3-propanesultone, and HDI were obtained from Alfa Aesar. 1,1,1,3,3,3-hexafluoro-2-propanol (HFIP) was obtained from Oakwood Chemical. PCL-diol, Sn(Oct)<sub>2</sub>, and 1,4-diaminobutane were dried in a vacuum oven prior to synthesis for removal of residual water.

Cells, Bacteria, and Viruses: Swine testicular (ST; ATCC CRL-1746) cells, CRFK (ATCC CCL-94) cells, and African green monkey kidney (Vero E6; ATCC NR-596) cells were purchased from the American Type Culture Collection (ATCC). Bacterial strains S. aureus (ATCC 6538), E. coli (CFT-73), MRSA (US300), VRE (clinical isolate), and a 14-strain bacterial cocktail were obtained from the Halomine Inc. (See Table S1, Supporting Information, for details). TGEV (ATCC VR-1740) and FCV (ATCC VR-782) were purchased from the ATCC. SARS-CoV-2 strain USA-WA1/2020 was obtained from BEI Resources (Manassas, VA, USA).

Synthesis of 3-((bis(2-hydroxyethyl)amino)methyl)-5,5-dimethylimidazolidine-2,4-dione: 5,5-dimethylhydantoin (26.4 g, 0.2 mol), diethanolamine (21.2 g, 0.2 mol), formaldehyde (16.2 g, 0.2 mol), and methanol (250 mL) were added to a 500 mL round-bottom flask. The mixture was stirred under a nitrogen atmosphere for 6 h at room temperature. After stirring, methanol and water byproducts were removed by rotary evaporation. The remaining viscous crude product was then dissolved in ethyl acetate, with anhydrous sodium sulfate added for further drying. After removal of sodium sulfate by filtration, the solution was refrigerated overnight. A white solid precipitate formed, which was collected and washed twice with cold ethyl acetate before further

purification via a silica gel column (eluent: DCM/methanol, 9:1 v/v). The chemical structure of the product (HA-diol) was confirmed by proton nuclear magnetic resonance.  $^1H$  NMR (DMSO-d<sub>6</sub>, 400 MHz, ppm):  $\delta$  8.28 (s, 1H), 4.37 (t, 2H), 4.30 (s, 2H), 3.42 (m, 2H), 2.63 (t, 2H), 1.28 (s, 6H).

Synthesis of 3-(butylbis(2-hydroxyethyl)ammonio)propane-1-sulfonate: N-Butyldiethanolamine (8.05 g, 0.05 mol), 1,3-propanesultone (6.7 g, 0.055 mol) and DCM (200 mL) were added to a 500 mL round-bottom flask. The mixture was stirred under a nitrogen atmosphere for 24 h at 40 °C. After stirring, the solvent was removed using a rotary evaporator. The product was precipitated by cold diethyl ether and then washed three times with cold diethyl ether to produce a white powder. The chemical structure of the product (SB-diol) was confirmed by proton nuclear magnetic resonance.  $^1$ H NMR (D<sub>2</sub>O, 400 MHz, ppm):  $\delta$  3.97 (t, 4H), 3.54 (m, 6H), 3.4 (t, 2H), 2.91 (t, 2H), 2.15 (m, 2H), 1.68 (m, 2H), 1.34 (m, 2H), 0.90 (t, 3H).

Synthesis of N,N-bis(2-hydroxyethyl)-N-methylbutan-1-aminium: N-Butyldiethanolamine (8.05 g, 0.05 mol), iodomethane (7.8 g, 0.055 mol), and anhydrous acetonitrile (250 mL) were added to a 500 mL round-bottom flask. The mixture was stirred under a nitrogen atmosphere for 24 h at 60 °C. After mixing, the solvent was removed by a rotary evaporator. The product was precipitated by cold diethyl ether and subsequently washed three times with cold diethyl ether to get a white powder. The chemical structure of the N,N-bis(2-hydroxyethyl)-N-methylbutan-1-aminium (N<sup>+</sup>-diol) was confirmed by proton nuclear magnetic resonance. <sup>1</sup>H NMR (D<sub>2</sub>O, 400 MHz, ppm):  $\delta$  4.07 (t, 4H), 3.60 (m, 4H), 3.46 (m, 2H), 3.19 (s, 3H), 1.78 (m, 2H), 1.41 (m, 2H), 0.97 (t, 3H).

Synthesis of HAPU: The HAPU was synthesized from PCL-diol, HA-diol, HDI, and 1,4-diaminobutane. Briefly, PCL-diol (10 g, 5 mmol) and HA-diol (3.9 g, 16 mmol) were dissolved in 250 mL anhydrous DMSO at 65 °C under nitrogen protection. HDI (4.04 g, 24 mmol) was then added to the flask dropwise, followed by the addition of two droplets of Sn(Oct)<sub>2</sub> catalyst. The mixture was stirred vigorously at 65 °C for 30 min. Then, 1,4-diaminobutane (0.26 g, 3 mmol) was added dropwise to the solution as a chain extender and stirred at 80 °C for 6 h. After the reaction, the viscous polymer solution was precipitated in DI water, and then washed three times with DI water. The resulting white powder (HAPU) was dried in vacuum at 60 °C.

Synthesis of SBPU: The SBPU was synthesized from PCL-diol, SB-diol, HDI, and 1,4-diaminobutane. Briefly, PCL-diol (10 g, 5 mmol) and SB-diol (4.5 g, 16 mmol) were dissolved in 250 mL anhydrous DMSO at 65 °C under nitrogen protection. HDI (4.04 g, 24 mmol) was then added to the flask dropwise, followed by the addition of two droplets of Sn(Oct)<sub>2</sub> catalyst. The mixture was stirred vigorously at 65 °C for 30 min. After mixing, the chain extender 1,4-diaminobutane (0.26 g, 3 mmol) was added dropwise to the solution, which was further stirred at 80 °C for 6 h. After the reaction, the viscous polymer solution was precipitated in diethyl ether, and then washed three times with diethyl ether. The resulting white powder (SBPU) was then washed three times with DI water and dried in vacuum at 60 °C overnight.

Synthesis of Quaternary Amine Based Polyurethane: The PU-N<sup>+</sup> was synthesized from PCL-diol, N<sup>+</sup>-diol, HDI, and 1,4-diaminobutane. Briefly, PCL-Diol (10 g, 5 mmol) and N<sup>+</sup>-diol (4.85 g, 16 mmol) were dissolved in 250 mL anhydrous DMSO solvent at 65 °C under nitrogen protection. HDI (4.04 g, 24 mmol) was then added to the flask dropwise, followed by two droplets of Sn(Oct)<sub>2</sub> catalyst. The mixture was stirred vigorously at 80 °C for 2 h. The chain extender 1,4-diaminobutane (0.26 g, 3 mmol) was then added dropwise to the solution and stirred at 80 °C for 6 h. After the reaction, the viscous polymer solution was precipitated in DI water, and then washed three times with DI water. The resulting white powder (PU-N<sup>+</sup>) was placed in vacuum oven at 60 °C overnight to remove the residual solvent.

Fabrication of the AVM: The AVMs were fabricated through an electrospinning process. Briefly, HAPU and SBPU polymers (mass ratio: 3:1) were dissolved in HFIP at 20% (w/v) at room temperature. The polymer solution was then loaded in a 20-mL plastic syringe (BD Biosciences) and injected at 2.4 mL  $h^{-1}$  by syringe pump (Harvard Apparatus, U.S.). The sub-micron fibers were spun at 15 kV with a 22G





www.afm-journal.de

blunt needle as the spinneret that was mounted on a robotic arm. The distance between the needle tip and the collector was set to 12 cm. The rotating aluminum rods (rotating speed: 400–450 rpm) or copper plate were covered with aluminum foil and placed in the path of the polymer solution jet to collect the electrospun fibers. After electrospinning, the membranes were peeled off from rod or aluminum foil, washed with DI water three times and dried in vacuum at room temperature to remove any residual solvent. The dried membranes were then cut into small pieces ( $1 \times 1 \text{ inch}^2$ ) with a weight of 30–34 mg and treated with 10% (v/v) household bleach solution (8.25% hypochlorite, pH adjusted to 7.0 with HCl) for 15 min or with 10% aqueous solution of NaDCC for 20 min to chlorinate the membranes. Subsequently, the chlorinated membranes were thoroughly washed with DI water and then dried to obtain the AVM.

Determination of Chlorine Content on the AVM: The immobilized chlorine content of AVM was determined using the iodometric/thiosulfate titration method. In brief, the AVM was immersed into 50 mL aqueous solution containing 1 mL of 0.1 mol  $L^{-1}$  acetic acid and 0.25 g potassium iodide. The mixture was then shaken at room temperature for 30 min to form  $\rm I_2$ . Drops of the 0.5% starch indicator solution was added until the sample turned blue. The mixture was titrated with a solution of 0.02 mol  $L^{-1}$  sodium thiosulfate until the sample turned from blue to colorless. The amount of immobilized chlorine content was calculated using the following formula:

$$[Cl\%] = 35.45 \times (C \times V)/2 W \times 100\%$$
 (1)

where Cl% is the weight percent of immobilized chlorine on the samples, C is the normality (mol  $L^{-1}$ ) of the titrant sodium thiosulfate solution, V is the volume (L) of the titrant sodium thiosulfate, and W is the weight (g) of the AVM, respectively.

The stability of chlorine on the AVM was evaluated under laboratory conditions (25 °C, 15–20% relative humidity) or aqueous solution. For each condition, triplicate membranes with the same size were stored for the predefined time period and titrated for immobilized chlorine content using the above-described iodometric/thiosulfate titration method.

To investigate the chlorine replenishment, the AVM was first chlorinated and titrated as described above. After the first chlorination and titration cycle, the samples were retrieved and washed thoroughly with DI water. This process was defined as one "chlorination—dechlorination" cycle (R1). This process was repeated nine additional times. The process of chlorination and titration was repeated with three parallel samples.

Material Characterizations: The tensile tests of the membranes were performed using an Instron 5965 and analyzed by the software Bluehill 3.0 SOP. The membranes were cut in a rectangular shape with 50 mm length, 10 mm width, and 2-3 mm thickness. The membranes were stretched until failure at a rate of 5 mm min<sup>-1</sup>. The fiber morphology of the membrane was characterized by scanning electron microscopy (SEM, LEO 1550). The pore size of the membranes was measured using an advanced capillary flow porometer (PMI CFP-1100-AEHXL) with a dry-wet method. Compressed air was used as the flowing gas and Silwick with 20.1 dynes cm<sup>-1</sup> surface tension was used as the wetting liquid to saturate specimens during the wet test. Surface elements of the membranes were analyzed using X-ray photoelectron spectroscopy (XPS). The hydrophilic properties of the membranes were characterized with contact-angle goniometer (ramé-hart). The molecular weights of the synthesized polyurethanes were tested by gel permeation chromatography GPC (Waters, USA).

Antimicrobial Efficacy Test: The antibacterial efficacy of AVM was evaluated against several model bacteria: gram-positive S. aureus, gramnegative E. coli, MRSA, VRE, and the army isolated cocktail of 14 strains. First, single colonies of each strain were picked from trypticase soy agar (TSA) plates, resuspended in brain–heart infusion medium, and cultured for  $16 \pm 4$  h at 37 °C on a shaking platform at 120 rpm rotation. The cultured bacteria were washed three times with Butterfield's phosphate buffer (BPB) after centrifugation (3000 rpm, 4 min). The bacterial suspensions were then adjusted to  $\approx 5 \times 10^7$  CFU mL $^{-1}$  using BPB. Twenty microliters of bacterial suspensions were inoculated on the

center of a  $1\times1$  inch sample to achieve an inoculum level of  $\approx1\times10^6.$  After 1, 15, or 30 min of contact, the samples were placed into 10 mL of  $Na_2S_2O_3$  solution (0.02 N) to quench any potential immobilized chlorines in the system, and vortexed for 5 min to detach any residual bacteria. Tenfold dilution series were performed and 20  $\mu L$  of every dilution were deposited on TSA plates. Bacteria were incubated at 37 °C for 24 h and viable bacterial colonies were counted and recorded. Each test was repeated three times.

Bacterial Attachment on the AVM: E. coli was used as a model strain to investigate bacterial attachment onto AVM. A hundred microliter of inoculum containing 10<sup>7</sup> CFU of E. coli were deposited on AVM samples for 30 min to allow attaching. Then, samples were gently rinsed with excess DI water before staining in Live/Dead Baclight Bacterial Viability Kit per manufacturer's instructions. The stained samples were imaged under an upright microscope (Zeiss Axioplan 2, Berlin, Germany). Five images from each sample were randomly captured, and the number of accumulated bacteria on the membranes were counted from captured images.

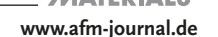
Antiviral Efficacy Test: The virucidal efficacy of AVM was tested against three model viruses: enveloped SARS-CoV-2, enveloped TGEV as a surrogate for the pathogenic human coronavirus such as SARS-CoV-1, and non-enveloped FCV as a surrogate for human norovirus.

ST cells and CRFK cells were maintained in Dulbecco's Modified Eagle's Medium (DMEM) supplemented with 1% penicillin–streptomycin (PenStrep) and 10% heat-inactivated fetal bovine serum (FBS) or horse serum, respectively, and incubated at 37 °C with 5%  $CO_2$ . TGEV and FCV were amplified in ST cell and CRFK cell cultures, respectively, to generate the working stocks. SARS-CoV-2 strain USA-WA1/2020 was obtained from BEI Resources (Manassas, VA, USA) and propagated to generate a working stock in Vero E6 cells. Vero E6 cells were cultured in complete cell culture media (DMEM supplemented with 5% FBS and 1% penicillin–streptomycin). To prepare the test samples, pieces of AVM were cut into  $1 \times 1$  inch squares with a weight of  $\approx 30-34$  mg. Melt blown polypropylene fabric (PPN) of N95 respirator (3M Model No. 1860, St. Paul, MN, USA) was cut into  $1 \times 1$  inch squares and used as control.

Inactivation of FCV and TGEV on AVM was tested by uniformly depositing 100 µL of viral stock at 10 different points on each sample. After 1-, 10-, 30-, and 120-min of contact, corresponding samples were immersed in 2.0 mL of DMEM medium and vortexed for 1 min to recover remaining virus. After vortex, the sample coupons were removed immediately from the liquid. The chlorine levels in the recovering media were confirmed to be below 0.5 ppm with chlorine testing strips (LaMotte 2979 Insta-TEST); the recovered virus suspensions were fivefold serially diluted. Viral infectivity titer before and after contact with samples was assessed by the TCID<sub>50</sub> method. Briefly, corresponding cells of FCV or TGEV were placed in 96-well plates and incubated until 70-80% confluent was reached. Each well of the 96-well plates were washed with PBS and infected with 100  $\mu L$  of corresponding dilutions with 6 replicates per dilution. The virus solutions were incubated with cell monolayers at 37 °C with 5% CO<sub>2</sub> for 1 h before addition of another 100 µL of cell culture media to reach complete cell media (DMEM supplemented with 1% PenStrep and 10% FBS for TGEV in ST cells, DMEM supplemented with 1% PenStrep and 10% horse serum for FCV in CRFK cells). The plates were incubated for 7 days to allow full CPE to develop. Subsequently, the plates were fixed with 10% paraformaldehyde solution for 1 h and stained with 1% crystal violet solution for 20 min. After a full wash with water, wells of the microtiter plate that were not stained by crystal violet were considered as infected by virus, and wells showing purple stain were considered as not infected by virus. The TCID<sub>50</sub> was calculated using the Reed-Muench method.<sup>[23]</sup>

SARS-CoV-2 tests were carried out by Battelle Memorial Institute, Columbus, OH, USA. All manipulations of SARS-CoV-2 were done in a biosafety level 3 (BSL-3) laboratory. SARS-CoV-2 inactivation on the AVM was examined as follows. Briefly, 100  $\mu L$  viral stock was uniformly distributed on 10 different points on each sample coupon. Melt-blown polypropylene fabric (PPN) of N95 respirator (3M Model No. 1860, St. Paul, MN, USA) was cut into 1  $\times$  1 inch squares and used as control. After 10-, 30-, or 120-min of contact, sample coupons were immersed in





10.0 mL of complete cell culture media, the same media used to maintain Vero E6 cells (DMEM supplemented with 5% FBS and 1% penicillinstreptomycin), and agitated on a platform shaker at 200 rotations per minute for 15 min to recover remaining virus. The extracts were then transferred to a concentrator (Spin-X UF Concentration, Corning Cat. No. CLS431491, Corning, NY) and centrifuged until the 10 mL starting volume was concentrated to  $\approx\!0.5$  mL. Complete cell culture media of Vero E6 cell was added to equilibrate all washed retentates to 2 mL. The sample retentates proceeded to the TCID $_{50}$  assay similar as abovementioned protocol for FCV and TGEV, with five replicates per dilution (N = 5). The 96-well plates were incubated 72 h before the determination for CPE on Vero E6 cell monolayers via visual inspection under microscope. Each sample was tested in triplicate (N = 3).

For all viral studies, whenever a sample that had less than three out of six wells showing virus positive (for FCV and TGEV) or three out of five wells showing virus positive (for SARS-CoV-2) at the lowest dilution factor, the titer was below LOD and value of LOD was assigned. The LOD of FCV and TGEV assays are 21 TCID $_{50}$ /sample or 1.32 log(TCID $_{50}$ /sample). The LOD of SARS-CoV-2 assay is 26.2 TCID $_{50}$ /sample or 1.42 log(TCID $_{50}$ /sample).

Cytotoxicity Test: The cytotoxicity of AVM was evaluated against NIH/3T3 Fibroblast, using the MTT cell proliferation assay. NIH/3T3 cells were first cultured in DMEM medium supplemented with 10% FBS and 1% penicillin–streptomycin. About  $1\times10^4$  cells were seeded into each 96-well TCPS plate for 24 h and then co-cultured with various concentrations (0.1–10 mg mL $^{-1}$ ) of unchlorinated and chlorinated AVM for 24 h at 37 °C. After incubation, 20  $\mu L$  of 5 mg mL $^{-1}$  MTT was added into each well and incubated under 37 °C for 4 h. Supernatant was then removed and 200  $\mu L$  DMSO was added to dissolve formazan crystals formed. Optical absorbance of the completely dissolved formazan solution was measured at wavelength of 570 nm using an absorbance microplate reader (BioTek, USA). Each sample was done in six replicates (n=6).

Water Filter Test: The bactericidal performance of AVM as a water filter was evaluated using a modified water filter method. AVM was first cut into circular shape to fit Nalgene analytical filter units.  $5 \times 10^5$  CFU of E. coli was then added to 10 mL of DI water and filtered through the analytical filter units under vacuum suction. After filtration, 10 mL of  $0.02~N~Na_2S_2O_3~solution~was~added~to~the~bacterial~suspension$ to quench any remaining immobilized chlorine and terminate any bactericidal action. Sterile polystyrene filter membranes with 0.22  $\mu m$ pore size were used as control. Bacterial dispersion was serially diluted and filtered through the control filter films. The AVM filter membranes were then divided into two triplicate groups: those from one group were put directly onto TSA plates and the rest were vortexed for 3 min to detach residual bacteria. The bacteria suspensions recovered from AVM and filtrates in the lower chamber were serially diluted and inoculated on TSA plates. After the TSA plates were incubated for 24 h at 37 °C, viable bacterial colonies were counted and recorded.

Statistical Analyses: Unless otherwise stated, data are expressed as mean  $\pm$  SEM in the experiments. One-way ANOVA were used to compare different groups of virus titer, followed by Tukey's post hoc test. The level of significance was labeled as NS, \*, \*\*, \*\*\*, and \*\*\*\*, denoting non-significant and p-values of <0.05, <0.01, <0.001, and <0.0001, respectively.

# **Supporting Information**

Supporting Information is available from the Wiley Online Library or from the author.

# **Acknowledgements**

The authors thank Prof. Luis M. Schang from the Department of Microbiology and Immunology of Cornell University for discussion of this work and Cornell Center for Materials Research Facility supported by the National Science Foundation under Award Number DMR-1719875 and Cornell NanoScale Science & Technology Facility supported by NSF

Grant NNCI-2025233 for providing equipment and expertise for material characterizations. This project was partially supported by the Hartwell Foundation, the Novo Nordisk Company, the US National Science Foundation (NSF) Small Business Innovation Research (SBIR; Grant No. 2028187 and 2014378) and National Institute of Allergy and Infectious Diseases of National Institutes of Health (NIH; Grant No. 1R43Al155114-01).

#### **Conflict of Interest**

M.M. and M.Q. are co-founders and shareholders of Halomine Inc. Y.Z. is an intern and M.Q. is an employee of Halomine Inc.

# **Author Contributions**

Q.L. and Y.Z. contributed equally to this work. Q.L., Y.Z., and M.M. conceived and designed the project, synthesized the materials, performed the experiments, and wrote the manuscript. Y.C. and M.F. performed SARS-CoV-2 tests. W.L. and L.W. contributed to the material characterizations. M.Q. contributed to experiment designs. V.B., L.W., K.S., and S.F. contributed to the discussions and preparation of the manuscript. All authors reviewed the manuscript and provided input.

# **Data Availability Statement**

Research data are not shared.

# **Keywords**

antiviral, N-halamine, SARS-CoV-2, sub-micron fibrous membranes, zwitterion

Received: April 13, 2021 Revised: June 25, 2021 Published online:

- a) R. Dehbandi, M. A. Zazouli, Lancet Microbe 2020, 1, e145;
  b) H. A. Aboubakr, T. A. Sharafeldin, S. M. Goyal, Transboundary Emerging Dis. 2021, 68, 296;
  c) N. Van Doremalen, T. Bushmaker, D. H. Morris, M. G. Holbrook, A. Gamble, B. N. Williamson, A. Tamin, J. L. Harcourt, N. J. Thornburg, S. I. Gerber, N. Engl. J. Med. 2020, 382, 1564.
- [2] a) WHO Coronavirus (COVID-19) Dashboard, https://covid19.who. int/ (Accessed: June 2021); b) J. A. Lewnard, N. C. Lo, Lancet Infect. Dis. 2020, 20, 631.
- [3] a) A. Berardi, D. R. Perinelli, H. A. Merchant, L. Bisharat, I. A. Basheti, G. Bonacucina, M. Cespi, G. F. Palmieri, Int. J. Pharm. 2020, 584, 119431; b) S. Ilyas, R. R. Srivastava, H. Kim, Sci. Total Environ. 2020, 749, 141652; c) S. Talebian, G. G. Wallace, A. Schroeder, F. Stellacci, J. Conde, Nat. Nanotechnol. 2020, 15, 618.
- [4] a) S. Behzadinasab, A. Chin, M. Hosseini, L. Poon, W. A. Ducker, ACS Appl. Mater. Interfaces 2020, 12, 34723; b) Long-Lasting Disinfection Evaluation Test Results, 2020, https://www.epa.gov/covid19-research/long-lasting-disinfection-evaluation-test-results-august-4-2020 (accessed: June 2021); c) Long-Lasting Disinfection Evaluation Test Results, 2020, https://www.epa.gov/covid19-research/long-lasting-disinfection-evaluation-test-results-august-10-2020 (accessed: June 2021); d) N. Baker, A. J. Williams, A. Tropsha, S. Ekins, Pharm. Res. 2020, 37, 104.
- [5] a) A. Dong, Y.-J. Wang, Y. Gao, T. Gao, G. Gao, Chem. Rev. 2017, 117, 4806; b) M. Qiao, Q. Liu, Y. Yong, Y. Pardo, R. Worobo, Z. Liu, S. Jiang, M. Ma, J. Agric. Food Chem. 2018, 66, 11441; c) Y. Ma,





- J. Li, Y. Si, K. Huang, N. Nitin, G. Sun, ACS Appl. Mater. Interfaces **2019**, 11, 17814; d) F. Wang, L. Huang, P. Zhang, Y. Si, J. Yu, B. Ding, Compo. Commun. **2020**, 22, 100487.
- [6] a) S. Jiang, Z. Cao, Adv. Mater. 2010, 22, 920; b) Q. Liu, A. A. Patel, L. Liu, ACS Appl. Mater. Interfaces 2014, 6, 8996.
- [7] J. M. Deitzel, J. Kleinmeyer, D. Harris, N. B. Tan, *Polymer* 2001, 42, 261.
- [8] C. Gehrke, J. Steinmann, P. Goroncy-Bermes, J. Hosp. Infect. 2004, 56, 49.
- [9] J. O. Akindoyo, M. Beg, S. Ghazali, M. Islam, N. Jeyaratnam, A. Yuvaraj, RSC Adv. 2016, 6, 114453.
- [10] a) G. A. Somsen, C. van Rijn, S. Kooij, R. A. Bem, D. Bonn, Lancet Respir. Med. 2020, 8, 658; b) L. Morawska, G. Johnson, Z. Ristovski, M. Hargreaves, K. Mengersen, S. Corbett, C. Y. H. Chao, Y. Li, D. Katoshevski, J. Aerosol Sci. 2009, 40, 256; c) K. A. Prather, C. C. Wang, R. T. Schooley, Science 2020, 368, 1422.
- [11] R. K. Campos, J. Jin, G. H. Rafael, M. Zhao, L. Liao, G. Simmons, S. Chu, S. C. Weaver, W. Chiu, Y. Cui, ACS Nano 2020, 14, 14017.
- [12] G. Cheng, H. Xue, Z. Zhang, S. Chen, S. Jiang, Angew. Chem. 2008, 120, 8963.
- [13] a) J. Choi, B. J. Yang, G.-N. Bae, J. H. Jung, ACS Appl. Mater. Interfaces 2015, 7, 25313; b) A. F. De Faria, F. Perreault, E. Shaulsky, L. H. Arias Chavez, M. Elimelech, ACS Appl. Mater. Interfaces 2015, 7, 12751.

- [14] a) S. M. Imani, L. Ladouceur, T. Marshall, R. Maclachlan, L. Soleymani, T. F. Didar, ACS Nano 2020, 14, 12341; b) A. M. Jastrzębska, A. S. Vasilchenko, ACS Sustainable Chem. Eng. 2021, 9, 601.
- [15] J. Doultree, J. Druce, C. Birch, D. Bowden, J. Marshall, J. Hosp. Infect. 1999, 41, 51.
- [16] D. H. Kingsley, E. M. Vincent, G. K. Meade, C. L. Watson, X. Fan, Int. J. Food Microbiol. 2014, 171, 94.
- [17] L. Casanova, W. A. Rutala, D. J. Weber, M. D. Sobsey, Water Res. 2009, 43, 1893.
- [18] a) Y. Sun, G. Sun, J. Appl. Polym. Sci. 2001, 80, 2460; b) B. Demir, R. M. Broughton, M. Qiao, T.-S. Huang, S. Worley, Molecules 2017, 22, 1582.
- [19] a) M. Qiao, T. Ren, T.-S. Huang, J. Weese, Y. Liu, X. Ren, R. Farag, RSC Adv. 2017, 7, 1233; b) J. Luo, N. Porteous, Y. Sun, ACS Appl. Mater. Interfaces 2011, 3, 2895; c) K. Xiu, J. Wen, N. Porteous, Y. Sun, J. Bioact. Compat. Polym. 2017, 32, 542.
- [20] Y.-H. Zhao, K.-H. Wee, R. Bai, J. Membr. Sci. 2010, 362, 326.
- [21] X. Dai, N. Sun, S. O. Nielsen, B. B. Stogin, J. Wang, S. Yang, T.-S. Wong, Sci. Adv. 2018, 4, eaaq0919.
- [22] B. Li, P. Jain, J. Ma, J. K. Smith, Z. Yuan, H.-C. Hung, Y. He, X. Lin, K. Wu, J. Pfaendtner, Sci. Adv. 2019, 5, eaaw9562.
- [23] L. J. Reed, H. Muench, Am. J. Epidemiol. 1938, 27, 493.